IJC
International Journal of Cancer

Immunogenomic analysis reveals *LGALS1* contributes to the immune heterogeneity and immunosuppression in glioma

Qun Chen[1†], Bo Han[1†], Xiangqi Meng[1], Chunbin Duan[1], Changxiao Yang[1], Zhenyu Wu[1], Dinislam Magafurov[1,2], Shihong Zhao[1], Shamil Safin[2], Chuanlu Jiang[1] and Jinquan Cai[1]

[1]Department of Neurosurgery, Second Affiliated Hospital of Harbin Medical University, Neuroscience Institute, Heilongjiang Academy of Medical Sciences, Harbin, China
[2]Department of Neurosurgery and Medical Rehabilitation ICPE, Bashkir State Medical University, Ufa, Russia

Mutualistic and dynamic communication between tumour cells and the surrounding microenvironment accelerates the initiation, progression, chemoresistance and immune evasion of glioblastoma (GBM). However, the immunosuppressive mechanisms of GBM has not been thoroughly elucidated to date. We enrolled six microenvironmental signatures to identify glioma microenvironmental genes. The functional enrichment analysis such as ssGSEA, ESTIMATE algorithm, Gene Ontology, Pathway analysis is conducted to discover the potential function of microenvironmental genes. *In vivo* and *in vitro* experiments are used to verify the immunologic function of *LGALS1* in GBM. We screen eight glioma microenvironmental genes from glioma databases, and discover a key immunosuppressive gene (*LGALS1* encoding Galectin-1) exhibiting obviously prognostic significance among glioma microenvironmental genes. Gliomas with different *LGALS1* expression have specific genomic variation spectrums. Immunosuppression is a predominate characteristic in GBMs with high expression of *LGALS1*. Knockdown of *LGALS1* remodels the GBM immunosuppressive microenvironment by down regulating M2 macrophages and myeloid-derived suppressor cells (MDSCs), and inhibiting immunosuppressive cytokines. Our results thus implied an important role of microenvironmental regulation in glioma malignancy and provided evidences of *LGALS1* contributing to immunosuppressive environment in glioma and that targeting *LGALS1* could remodel immunosuppressive microenvironment of glioma.

Introduction

Gliomas are the most common primary tumours in the central nervous system (CNS). Patients suffering from GBM survive on average no more than 15 months though maximal resection.[1] The tumour microenvironment (TME) forms an integral part of these tumours, and it is necessary to establish a dynamic

Key words: microenvironment, glioblastoma, *LGALS1*, prognosis, immunosuppression

Abbreviations: APC: antigen-presenting cell; CGGA: Chinese Glioma Genome Atlas; CNS: central nervous system; CNV: copy number variation; GBM: glioblastoma; GSEA: gene Set Enrichment Analysis; MDSC: myeloid-derived suppressor cell; PCA: principal components analysis; ssGSEA: single-sample GSEA; TCGA: The Cancer Genome Atlas; TME: tumour microenvironment

Additional Supporting Information may be found in the online version of this article.

†Q.C. and B.H. contributed equally to this work

Conflict of interest: The authors declare that they have no competing interests.

Authors' contributions: Jinquan Cai and Chuanlu Jiang devised the project, the main conceptual ideas and proof outline. Qun Chen and Bo Han conducted the most data analysis and experiments and prepared the study; other authors performed some experiments for our study. All authors read and approved the final study.

Grant sponsor: The National Key Research and Development Plan; **Grant number:** No. 2016YFC0902500; **Grant sponsor:** The National Natural Science Foundation of China; **Grant numbers:** No. 81702972, No. 81874204, No. 81572701, No. 81772666; **Grant sponsor:** China Postdoctoral Science Foundation; **Grant number:** 2018M640305; **Grant sponsor:** The Research Project of the Chinese Society of Neuro-oncology, CACA; **Grant number:** CSNO-2016-MSD12; **Grant sponsor:** The Research Project of the Health and Family Planning Commission of Heilongjiang Province; **Grant number:** 2017-201; **Grant sponsor:** The Harbin Medical University Scientific Research Innovation Fund; **Grant number:** 2017LCZX37

DOI: 10.1002/ijc.32102

History: Received 12 Sep 2018; Accepted 20 Dec 2018; Online 7 Jan 2019

Correspondence to: Jinquan Cai, Department of Neurosurgery, Second Affiliated Hospital of Harbin Medical University, Neuroscience Institute, Heilongjiang Academy of Medical Sciences, Harbin, China, E-mail: caijinquan666777@126.com; or Chuanlu Jiang, Department of Neurosurgery, Second Affiliated Hospital of Harbin Medical University, Neuroscience Institute, Heilongjiang Academy of Medical Sciences, Harbin, China, E-mail: jcl6688@163.com

What's new?

When a glioblastoma (GBM) develops in the CNS, immunosuppressive cytokines allow the tumor to evade and suppress the immune system. They also prevent current immunotherapies from effectively attacking the tumor. In this study, the authors found that variations in the gene coding for the cytokine Galectin-1 may provide a prognostic biomarker in GBM. They also found that blocking this gene reduces immunosuppression in the GBM microenvironment. These results help to explain why immunosuppression is a hallmark of GBMs, and may also lead to improved immunotherapies for this aggressive tumor.

interaction with tumour cells. This interaction, in turn, influences tumour growth, chemoresistance and immune evasion.

Immune evasion and suppression is an important factor in preventing current immunotherapies from effectively fighting against GBM. Immunosuppressive microenvironment within the tumours facilitates the growth and malignant properties of the lesion while evading the body's immune system.[2] Therefore, there is significant value in discovering potential immunosuppressive features in GBM.

The finding of the lymphatic system[3] in the CNS has inspired researchers to explore the therapeutic methods based on tumour immunity. The uniquely immune-privileged microenvironment due to inherent expression of immunosuppressive cytokines, such as Galectin-1,[4] PD-1, TGF-β and IL10, and lack of antigen-presenting cells (APCs) in the CNS poses an obstacle for the efficacy of immunotherapy in GBM.[5] Therefore, the development of new therapies with improved activity at the tumour site will require a deeper understanding of the tumour immunosuppressive microenvironment in GBM. Galectin-1 encoded by *LGALS1* is a member of beta-galactoside-binding protein family, involved in the homeostasis of the immune system, tumour cell growth and the interaction between cell–cell and cell–matrix.[6] Galectin-1 is highly secreted in a variety of tumours[7] and plays an important role in the negative regulation of immune responses.[8] T cell activity is heightened after the inhibition of Galectin-1 in tumours, which indicates that Galectin-1 is a determining factor in tumour-immune privilege.[9]

However, the immunomics alternation of *LGALS1* is poorly understood in GBM microenvironment. Deeply analysing the population-based samples, investigating the characteristic of immunosuppressive biological process of *LGALS1* based on current transcriptome databases may help to resolve the immune complexity of GBM and guide potential anti-*LGALS1* therapy.

In the present study, we employed 2,360 glioma samples to investigate the microenvironmental biological processes, explore the immunomics alternation, clinicopathologic characterization of *LGALS1* expression in glioma, and clarify the contribution of *LGALS1* to immunosuppressive microenvironment of glioma *in vivo*.

Materials and Methods

Glioma patient databases

Five types of mRNA databases from patients were used from Chinese Glioma Genome Atlas (CGGA) database (microarray, n = 310) (http://www.cgga.org.cn), The Cancer Genome Atlas (TCGA) database (microarray, n = 539, RNAseq, n = 702) (http://cancergenome.nih.gov/), the Rembrandt database (microarray, n = 475) (https://caintegrator.nci.nih.gov/rembrandt/), the GSE16011 database (microarray, n = 284) and the GSE43378 database (microarray, n = 50). DNA copy number and mutation profiles were obtained from the TCGA website (http://cancergenome.nih.gov/).

Cell culture and xenograft mouse tumours

GL261 and BV2 cells were maintained in Dulbecco's modified Eagle's medium (DMEM) supplemented with 10% Foetal Bovine Serum (FBS), 2 mM l-glutamine, and 1% penicillin–streptomycin (Solarbio, China). Six- to seven-week-old female wild-type C57BL/6 mice were purchased from the Chinese Academy of Medical Science (Beijing, China) Animal Centre and housed in conventional pathogen-free conditions. Thirty mice were used in our study and each group was ten mice. Briefly, 5×10^5 GL261 cells were infected with lenti-si*LGALS1* (GeneChem, Shanghai, China) and stereotactically injected into mouse brains using cranial guide screws. Sequences: siRNA1 5′-ACCUGUGCCUACACUUCAA-3′, siRNA2 5′-ACUUGAAUUCGUAUCCAUCUG-3′ and scrambled siRNA 5′-GGAAAUCCCCCAACAGUGA-3′ were purchased from GeneChem (Shanghai, China).

Immunohistochemistry

We obtained paraffin-embedded glioma tissues from patients who provided informed consent under an Institutional Ethics Committee-approved study from the Second Affiliated Hospital of Harbin Medical University. The immunohistochemistry (IHC) assay was carried out according to our previous research.[10] The slices were incubated with primary antibodies Galectin-1 (CST, 1:250), VEGFA (BOTSER, 1:200), CCL2 (Proteintech, 1:100), TGF-β (abcam, 1:100), CD68 (BOTSER, 1:50), CD163 (Proteintech, 1:50) and CD11b (CST, 1:200). For quantitative evaluation was performed by examining each slice using at least three different high-power fields with the most abundant areas as our previous research described.[11] The staining scores of cytokines were classified into six categories (0–5) based on the staining intensity.[12] For the stained cells, staining was scored using a 4-point scale from 0 to 3, with "0" if there was no staining or very little staining, "1" if less than 10% of cells stained positively, "2" if 10%–30% of cells stained positively, and "3" if more than 30% of cells stained positively.[13]

Flow cytometry

Flow cytometry was conducted according to standard protocols. In brief, brain tumours were stripped and perfused with PBS. Single cell suspensions were obtained after mincing with scalpels and 30 min incubation with DNase (Invitrogen) and Collagenase D (Roche). M2 macrophage and MDSC cells from tumour tissues were stained with fluorochrome conjugated mAbs for 30 min on ice in the presence CD163/CD68, CD11b/Gr-1. Flow cytometric analysis was performed with FlowJo software.

Enzyme-linked immunosorbent assay

Enzyme-linked immunosorbent assay (ELISA) quantification of Galectin-1, CCL2, VEGFA and TGF-β in the culture medium of GL261 cells were performed using the human Galectin-1, CCL2, VEGFA and TGF-β ELISA Kit (Sigma-Aldrich) following manufacturer's instructions. Culture medium was diluted up to 50 times as appropriate for each cytokine, and concentrations were normalized per mL/1 × 10^6 cells.

Immunoblotting

Western blot (WB) and immunofluorescence (IF) assays were performed as previously described.[14] Primary antibodies mouse Galectin-1 (CST, 1:1000), mouse anti-GAPDH (1:1000, ABclonal) were used along with horseradish peroxidase-labeled secondary antibody (1:10000, sigma) in WB. CD68 (1:50, Santa Cruz), CD163 (1:100, Santa Cruz), CD204 (1:50, Santa Cruz) and CD206 (1:50, Santa Cruz) were used for IF.

Invasion, soft agar colony formation, and colony formation assays

For the soft agar assay, 24-well plates were pre-coated with 0.5 mL 1 × concentration complete 1,640 medium (Gibco, Gaithersburg, MD, USA) containing 0.6% agarose (Yeason) with 10% FBS. Cells were suspended in 1 mL complete 1,640 medium with 0.35% agarose. Fully-suspend cells were placed into the upper layer and incubated at 37 °C with 5% CO2 for 3 weeks. Cell colonies were stained with 0.1% crystal violet for 5 min and observed using a Bio-Rad ChemiDoc™ imaging system (Berkeley, CA, USA). For colony formation assay, 6-well plates were seeded with 300 cells as indicated. The assay was stopped when the colonies could be observed with the naked eye. Then, cells were fixed with methanol 4% and stained with 0.1% crystal violet for recording colony numbers. The invasion assay was performed in 24-well cell culture chambers with transwell inserts (Corning) precoated with Matrigel. In brief, 1 × 10^4 GBM cells were seeded per chamber. After 36 h, the lower surfaces of chambers were fixed with 4% methanol for 5 min and stained with 0.1% crystal violet. All experiments were performed in triplicate.

Statistical analysis

Student's *t*-test and one-way analysis of variance (one-way ANOVA) were used to assess differences in the variable groups. Survival analysis was conducted by using the Kaplan–Meier curves and the log-rank test through the GraphPad Prism 7 software. Gene ontology (GO) was carried out when gene sets (Pearson r > 0.4) were uploaded to the DAVID website (http://david.abcc.ncifcrf.gov/home.jsp). ClueGO, a Cytoscape version 3.3.0 with the extension app ClueGO[15] was used to process the pathway analysis. Gene Set Enrichment Analysis (GSEA) was performed to identify groups of genes enriched in either high or low *LGALS1* groups.[16] "Estimation of STromal and Immune cells in Malignant Tumours using Expression data" (ESTIMATE) was used to calculated levels of infiltrating stromal, immune cells and tumour purity in tumour samples.[17] Single-sample GSEA (ssGSEA) analysis, which calculates separate enrichment scores for each pairing of a sample and gene set[18] was used to assess the gene score of every gene set for every sample. R version 3.3.2 with the extension package "circlize"[19] and "ComplexHeatmap", and "circus"[20] were used to produce figures. Heatmaps were generated using the Gene Tree View software. The principal components analysis (PCA) and ROC were performed by using the SPSS 22.0. Statistical values of $p < 0.05$ were considered to be significant.

Results

Identification of eight glioma microenvironmental genes through the functional enrichment analysis for glioma databases

To investigate the underlying molecules involved in glioma microenvironment, we built six glioma microenvironment signatures containing mature vascular signature (Mature vascular), microvascular signature (Microvascular), hypoxia activation signature (Hypoxia activation),[21] tumour purity, stromal and immune scores.[17]

We performed the single-sample ssGSEA[18] or ESTIMATE algorithm[17] for the selected six glioma microenvironment signatures to generate corresponding scores that reflect the presence of each gene signature in the glioma samples.

Next, we used the Pearson correlation analysis to excavate the genes correlated with the Mature vascular score, Microvascular score, Hypoxia activation score, stromal score, immune categories score (r > 0.65) and tumour purity score (r < −0.65) in the TCGA, CGGA, Rembrandt and GSE16011 databases (Fig. 1*a-d*). We overlapped the above 4 positively correlated genelists and obtained eight glioma microenvironmental genes: *CCDC109B*, *EMP3*, *ANXA2*, *CLIC1*, *TIMP1*, *VIM*, *LGALS1* and *RBMS1*.

Glioma microenvironmental gene scores have specific genomic and transcriptomic spectrums in glioma samples

Based on expression data, another ssGSEA score for the eight gene group was calculated, called the glioma microenvironmental gene score, for comparison with CNV and mutation data. We defined the median of glioma microenvironmental genes score as the cutoff point to separate the samples into those with high or low glioma microenvironmental genes score. We observed amplification events of chromosome 7 and deletion events of chromosome 10 were enriched in

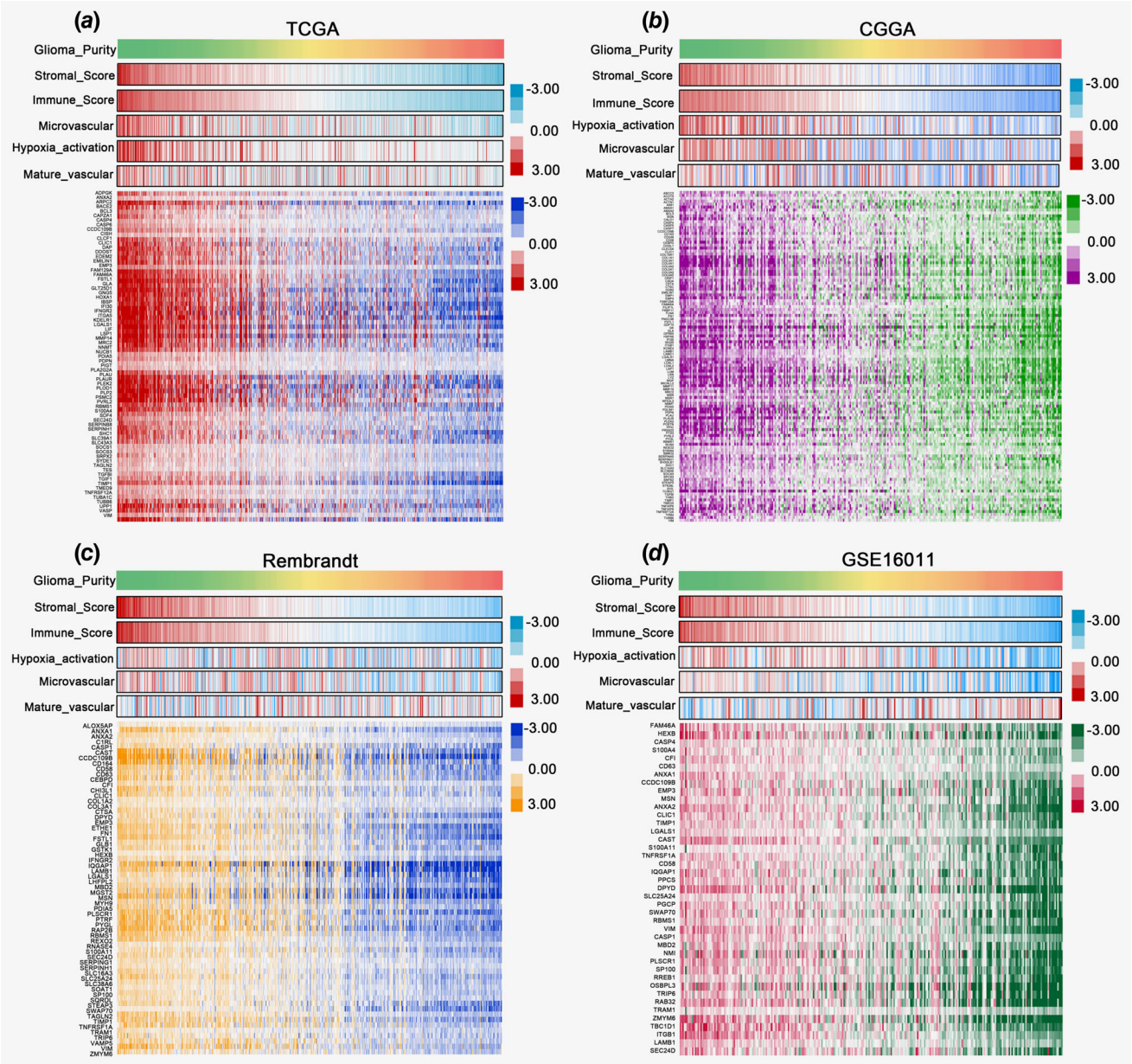

Figure 1. The transcriptomic alternation of glioma microenvironment signatures in glioma databases. (*a-d*) Heatmaps of genes correlated with glioma microenvironment signatures of glioma purity, stromal score, immune score, hypoxia activation, microvascular and mature vascular signatures in the TCGA, CGGA, Rembrandt and GSE16011 databases. [Color figure can be viewed at wileyonlinelibrary.com]

samples with high glioma microenvironmental gene score. However, 1p/19q deletion events were observed in samples with low glioma microenvironmental gene score (Fig. 2*a-b*). Pearson correlation analysis was used to explore the relationship between the copy number of chromosomal regions and the glioma microenvironmental gene score. The genomic sites of chr1p, chr7, chr10 and chr19q were most highly correlated with the glioma microenvironmental gene score ($|r| > 0.3$, Fig. 2*c*, Supporting Information Fig. S1A-D).

In detail, we found that high *EGFR* amplification (33%) and *PTEN* (6%) deletion rates occurred in samples with high glioma microenvironmental gene score (Fig. 2*d*). High mutation rates of in *IDH* (92%), *ATRX* (38%), *CIC* (23%), *FUBP1* (13%) and *NOTCH1* (8%) were observed in samples with low glioma microenvironmental gene score. In contrast, high rates of *EGFR* (19%) and *PETN* (18%) mutations occurred in samples with high glioma microenvironmental gene score (Fig. 2*e*). We did PCA after considering the Mature vascular score, Microvascular score, Hypoxia activation score, tumour purity score, stromal score and immune score. PCA1 and PCA2 represented the top two dimensions showing a good separation between the groups with low and high glioma microenvironmental gene score in

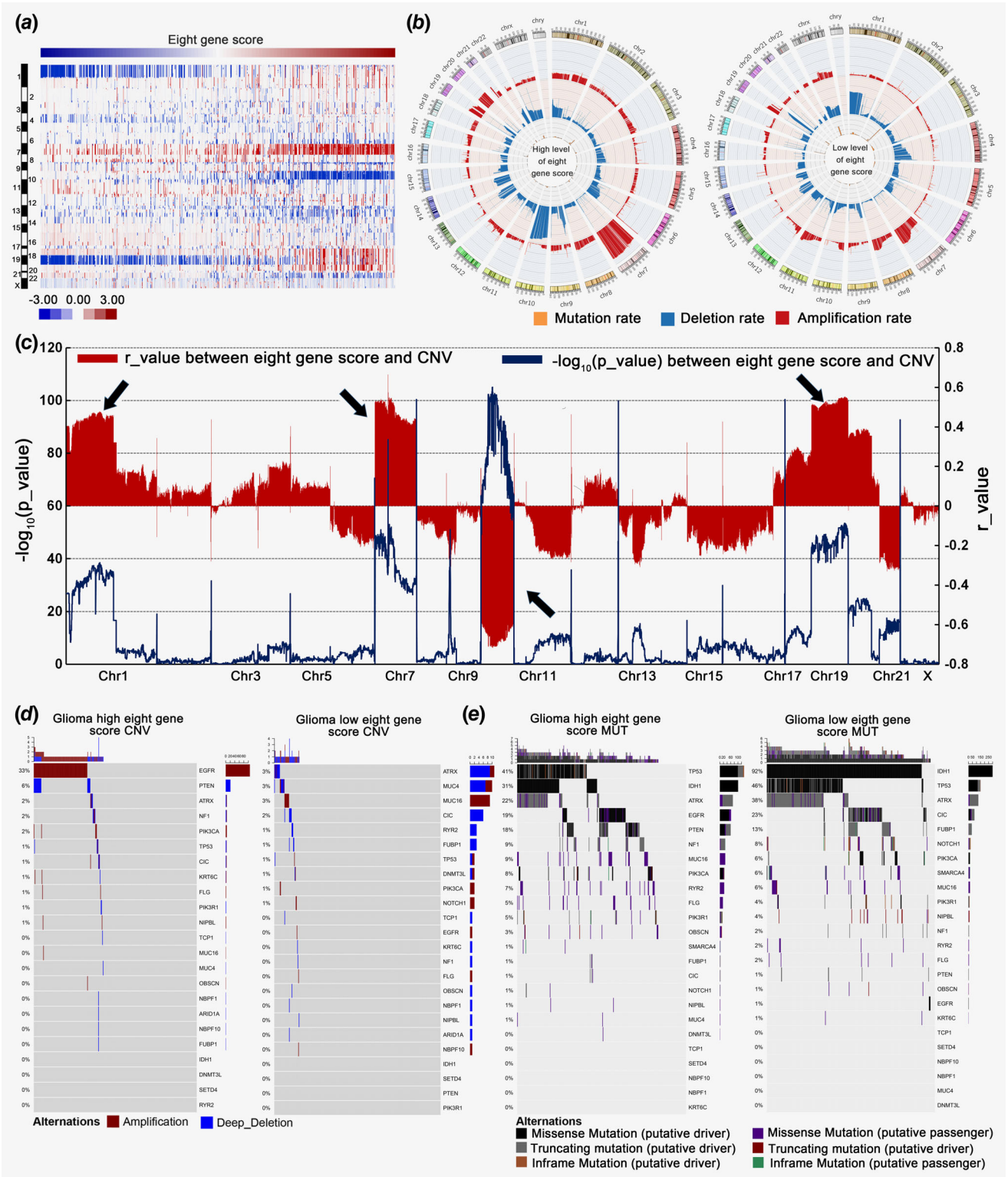

Figure 2. Low and high glioma microenvironmental gene scores have different specific genomic and transcriptomic spectrums in glioma samples. (*a*) CNV spectrum with increasing glioma microenvironmental gene score. (*b*) The circos plot presented the incidence of deletion (blue), amplification (red) and mutation (orange) rates in chromosomes. (*c*) The plot of Pearson correlation results (r and *p* values) with arrows highlighting the regions with peak correlations between the copy number of chromosomal regions and the glioma microenvironmental gene scores. (*d*) CNV were visualized by comparing gliomas with low and high glioma microenvironmental gene score. (*e*) Somatic mutation spectrums were visualized by comparing gliomas with low and high glioma microenvironmental gene score. [Color figure can be viewed at wileyonlinelibrary.com]

the TCGA (63.46%, 17.21%), CGGA (62.74%, 15.29%), Rembrandt (51.97%, 21.49%) and GSE16011 (60.85%, 17.12%) databases (Supporting Information Fig. S2A-D).

Next, we investigated microenvironmental gene score according to the WHO classification grade system, histopathology and *IDH* mutation status. We found that the score level of glioma microenvironmental genes was the highest in WHO IV glioma (TCGA p = 7.646E-120, CGGA p = 2.923E-38, and Rembrandt p = 6.391E-40), GBM (TCGA p = 2.726E-122, CGGA p = 1.338E-41, and Rembrandt p = 6.391E-40) and *IDH* wild-type GBM (TCGA p = 5.805E-11, and CGGA p = 3.986E-13, Supporting Information Fig. S3A-C). Next, we inspected the score level of glioma microenvironmental genes among the different molecular subtypes defined by the TCGA network.[22] The highest score level was observed in mesenchymal subtype in the TCGA (p = 1.235E-18), CGGA (p = 6.219E-18) and Rembrandt (p = 5.393E-39) databases (Supporting Information Fig. S3D-F). ROC curves for the score level of glioma microenvironmental genes and mesenchymal subtype of all GBM subtypes were analysed. The area under the curve (AUC) values were 81.13%, 82.95% and 83.56% (Supporting Information Fig. S3G) in the TCGA, CGGA and Rembrandt databases, respectively (Supporting Information Fig. S3H-I).

LGALS1 reveals obviously prognostic significance among glioma microenvironmental genes and shows its malignant biological phenotype in glioma

To further evaluate the prognostic value among the eight glioma microenvironmental genes, we found that *CLIC1*, *LGALS1*, *TIMP1*, *CCDC109B*, *ANXA2*, *EMP3* and *RBMS1* in the TCGA database had statistical significance ($p < 0.05$) using Cox regression analysis. We also validated these findings in the CGGA, Rembrandt, GSE16011 and GSE43378 (Supporting Information Tables S1-S5). We overlapped significantly prognostic genes among five databases (Supporting Information Fig. S4A), and found that *CCDC109B, EMP3, LGALS1* revealed prognostic significance. However, according to the hazard ratio score as a ratio of death probabilities,[23] we found that *LGALS1* revealed the highest level in TCGA, Rembrandt and GSE43378 databases (Supporting Information Fig. S4B). We used dichotomization to separate cases for depicting the survival curves according to the best cutoff point. Low expression of *LGALS1* resulted in a significantly longer overall survival time (TCGA median survival time: 395 days; CGGA median survival time: 561 days) than high expression of *LGALS1* (TCGA median survival time: 313 days; CGGA median survival time: 403 days) (Fig. 3*a*). In a multivariate Cox proportional hazards model, the *IDH1* status, TCGA subtype, level of *LGALS1*, age at diagnosis and chemotherapy category were all associated with overall survival in the TCGA and CGGA databases (Fig. 3*b*). Knockdown of *LGALS1* (Fig. 3*c*) supressed soft cell invasion, proliferation, colony formation and soft agar colony formation (Fig. 3*d-g*).

LGALS1 is preferentially expressed in the mesenchymal subtype of GBM

LGALS1 expression differed significantly in WHO grade, histology and *IDH* status (Fig. 4*a-c*). The highest expression was observed in GBM (WHO IV). *IDH1* wild-type glioma presented with higher *LGALS1* expression than *IDH1* mutant glioma. In glioma tissues, we found that the protein level of Galectin-1 was highest in GBM (Fig. 4*d*). *LGALS1* expression also differed significantly among molecular GBM subtypes. The highest expression was observed in the mesenchymal subtype of the TCGA (p = 1.454E-35), CGGA (p = 4.582E-12) and Rembrandt (p = 6.219E-41) databases (Fig. 4*e-g*). ROC curves for *LGALS1* expression and the mesenchymal subtypes were analysed in GBM. The AUC values were 74.00%, 82.95% and 83.56% in the TCGA, CGGA and Rembrandt databases, respectively (Fig. 4*h*). Similarly, the GSEA between the different groups demonstrated that mesenchymal gene set was enriched in patients with high levels of *LGALS1* in the TCGA, CGGA and Rembrandt databases (Fig. 4*i-k*).

Gliomas with different *LGALS1* expression have specific genomic variation spectrums

Next, we used the TCGA CNV and somatic mutation databases to investigate the relationship among the level of *LGASL1*, the copy number and the mutation levels. High levels of *LGALS1* were accompanied with amplification events of chromosome 7 and deletion events of chromosome 10 (Supporting Information Fig. S5A-B). Pearson correlation analysis was used to explore the relationship between the copy number of chromosomal regions and the level of *LGALS1* expression. The genomic sites of chr1p, chr7, chr10 and chr19q were most highly correlated with the level of *LGALS1* expression ($|r| > 0.3$, Supporting Information Fig. S5C-G). *EGFR* amplifications (32%) and *PTEN* (6%) deletions were more likely to observed at high levels in the high *LGALS1* group (Supporting Information Fig. S6A). Overall, mutations in *EGFR* (19%) and *PETN* (19%) occurred at the high *LGALS1* group. The most common mutations were in *IDH1* (91%), *TP53* (55%), *ATRX* (45%), *CIC* (18%) and *FUBP1* (10%), all of which were correlated with the low *LGALS1* group (Supporting Information Fig. S6B).

LGALS1 is involved in immunologic biological processes, associated with immunosuppressive signalling pathway

To further delineate the common principles of the biological processes associated with *LGALS1*, we selected the genes that correlated with *LGALS1* expression (Pearson $r > 0.4$). Next, we performed the GO analysis of the genes that were positively correlated with *LGALS1* in the TCGA, CGGA and Rembrandt databases. Most prominent in the results of GO analysis were terms ($p < 0.05$) describing leukocyte migration, chemotaxis, innate immune response and interferon-gamma-mediated signalling pathway in the TCGA database (Supporting Information Fig. S7A). In the CGGA database, GO terms, such as antigen processing, chemotaxis, inflammatory response, leukocyte

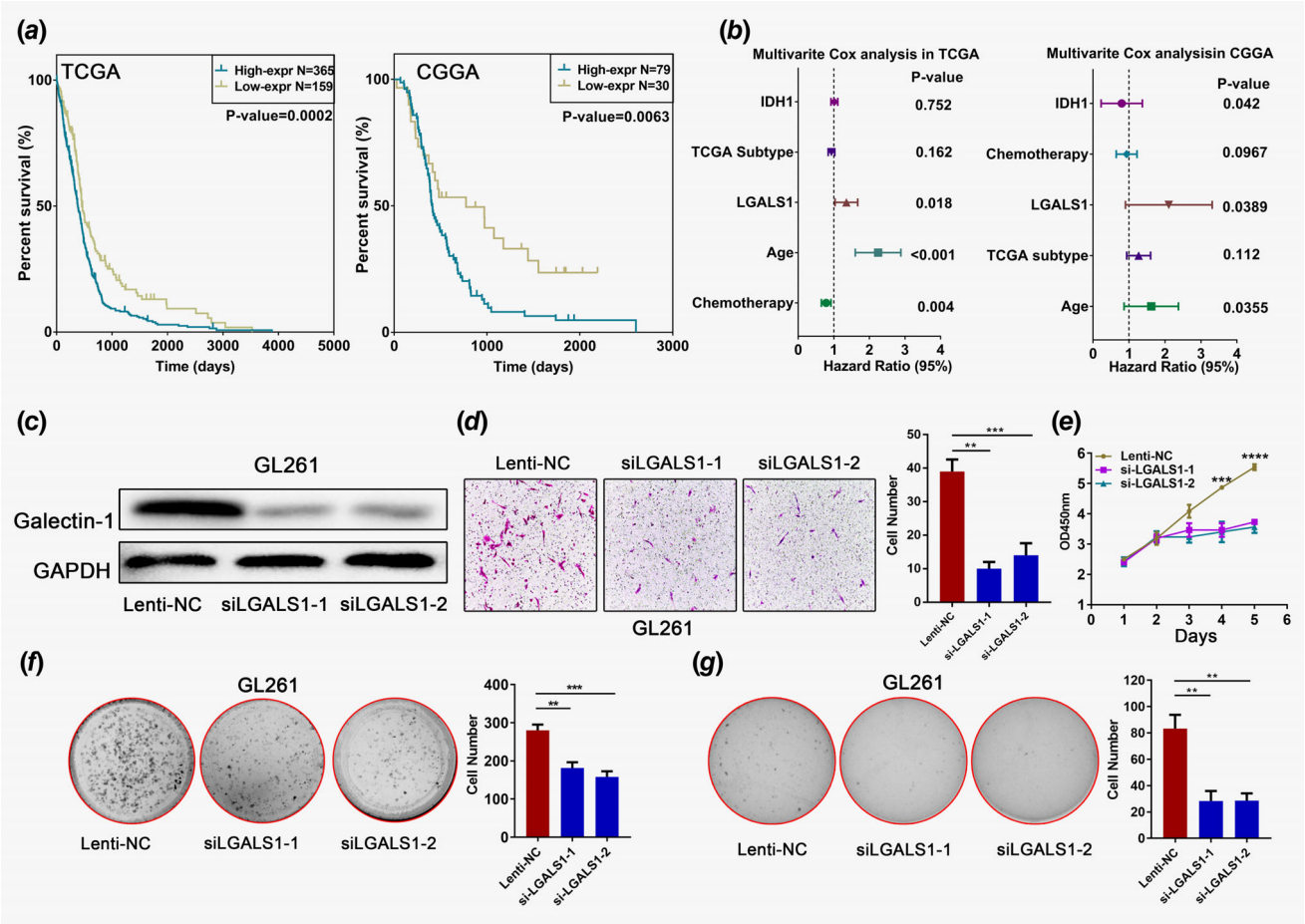

Figure 3. *LGALS1* reveals its obviously prognostic significance in GBM and its malignant biological phenotypes *in vitro*. (*a*) Patients with a low level of *LGALS1* lived significantly longer than patients with a high level of *LGALS1* in the TCGA and CGGA. (*b*) The multivariate Cox proportional hazards model was conducted using backward stepwise selection of variables based on *IDH1* status, TCGA subtypes, the level of *LGALS1*, the age at diagnosis and whether chemotherapy was received in the TCGA and CGGA databases. (*c*) Western blot analysis validated the knockdown of *LGALS1* in GL261 cells. (*d*) Transwell invasion assay was performed to evaluate the invasion ability after knockdown of *LGALS1*. (*e*) CCK8 assay was performed to evaluate the proliferative ability after knockdown of *LGALS1*. (*f*, *g*) Colon and soft agar formation assays were performed to evaluate the proliferative ability after knockdown of *LGALS1*. * $p < 0.05$, ** $p < 0.01$, *** $p < 0.001$, **** $p < 0.0001$. [Color figure can be viewed at wileyonlinelibrary.com]

migration and innate immune response, were enriched in the high *LGALS1* group (Supporting Information Fig. S7B). Besides the immune response and TRIF-dependent toll-like receptor signalling pathway, similar patterns could be observed in the Rembrandt database (Supporting Information Fig. S7C). GSEA further confirmed that high level of *LGALS1* was related to the innate immune response, immune response, immune system process and negative regulation of the immune system process in the TCGA, CGGA and Rembrandt databases (Supporting Information Fig. S8A-C). We overlapped the genes positively related to *LGALS1* among the TCGA, CGGA and Rembrandt databases and obtained 376 genes (Supporting Information Table S6). Pathways analysis was performed by using these genes, and the results were visually graphed by Cytoscape. Network representation of the *LGALS1*-associated pathways revealed that neutrophil degranulation, interleukin-6 signalling, interleukin-10 (IL-10) signalling and immunoregulatory interactions between a lymphoid and a non-lymphoid were involved (Supporting Information Fig. S8D). We also assessed the immune metagenes.[24] As shown in Supporting Information Figure S9A-C, after the metagenes were calculated through ssGSEA, we found that *LGALS1* was positively related to HCK (hemopoietic cell kinase), LCK (lymphocyte-specific kinase), MHC_I (major histocompatibility complex I), MHC_II (major histocompatibility complex II), STAT1 (signal transducer and activator of transcription 1), and Interferon (Supporting Information Tables S7-S9). However, *LGALS1* was negatively related to IgG (Supporting Information Tables S7-S9). In the meantime, we parsed the gene sets of immune cells (Supporting Information Fig. S10A-C and Tables S10-S12) and found that helper T-cells, cytotoxic T-cell, monocytes, CD19 B cells, myeloid cells, natural killer cells, dendritic cells, T-cell lineages and myeloid lineages were all positively correlated with the level of *LGASL1*.

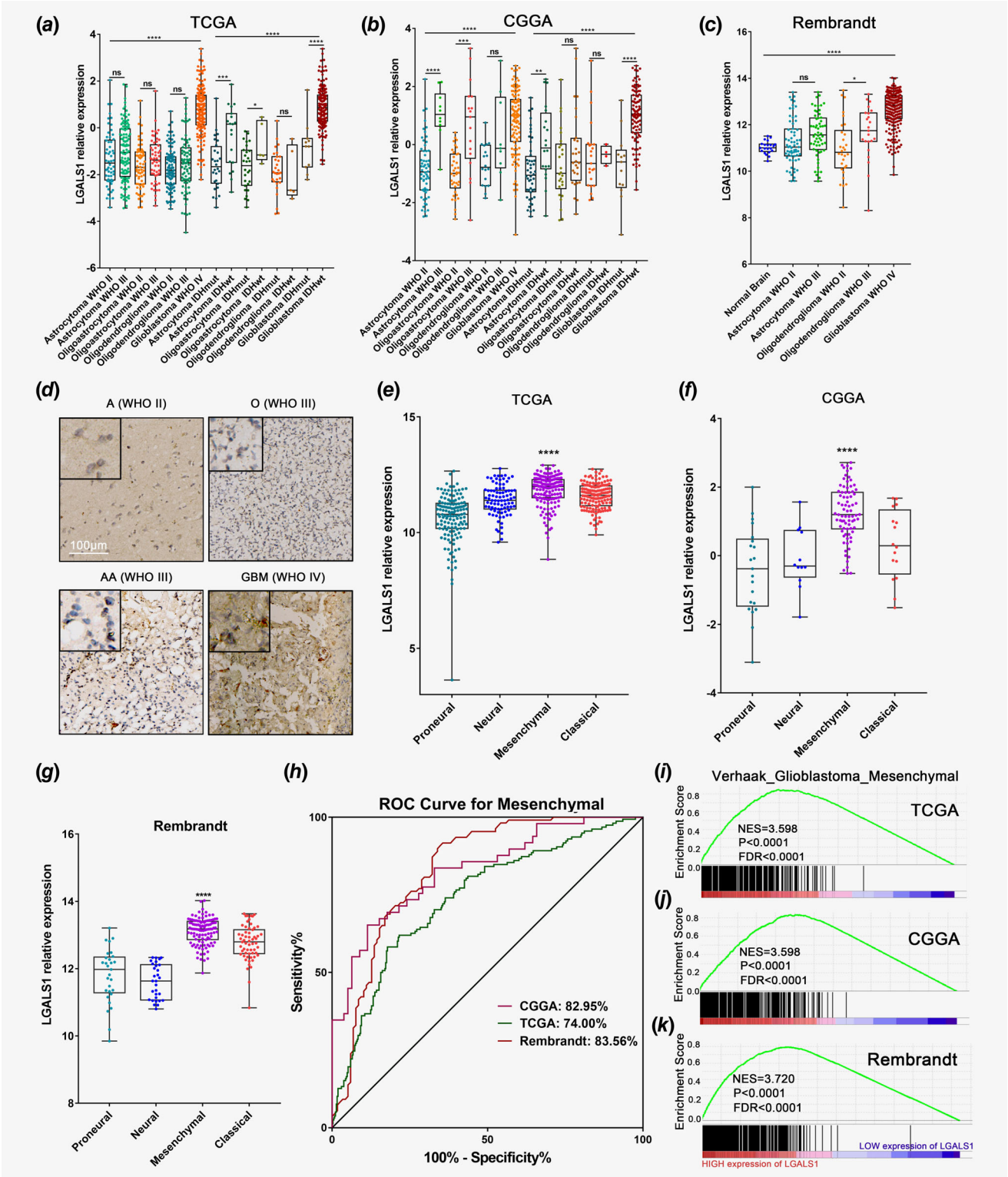

Figure 4. *LGALS1* is preferentially expressed in the mesenchymal subtype of GBM. (*a–c*) The distribution patterns of *LGALS1* according to WHO, histopathology and molecular pathology classifications in the TCGA, CGGA and Rembrandt databases. (*d*) The immunohistochemical analysis showed that *LGALS1* was increased in GBM. Scale bar 100 μm. (*e–g*) The distribution patterns of *LGASL1* in different subtypes in the TCGA, CGGA and Rembrandt databases. (*h-k*) ROC curve and GSEA analysis indicated that *LGALS1* could predict the mesenchymal subtype in TCGA, CGGA and Rembrandt databases. * $p < 0.05$, ** $p < 0.01$, *** $p < 0.001$, **** $p < 0.0001$. [Color figure can be viewed at wileyonlinelibrary.com]

Immunosuppression is a predominate characteristic in GBMs with high expression of *LGALS1*

As revealed above, *LGALS1* plays a role in immunosuppression in GBM. Next, we parsed the TCGA, CGGA and Rembrandt databases to show that the proportion of patients with high *LGALS1* levels also had a significantly higher correlation with glioma-mediated immunosuppressive metagenes[4,11] (Fig. 5*a-c* and Supporting Information Tables S13-S15), such as Markers of Tregs, Immunosuppressive signalling pathways, tumour-supportive macrophage chemotactic and skewing molecules, Immunosuppressive cytokines and checkpoints, and immunosuppressors. These results implied that *LGALS1* played a role in immunosuppression of GBMs. Next, we overlapped *LGALS1*-positive related genes from the TCGA, CGGA and Rembrandt databases with immunosuppressive metagenes and obtained 13 effectors. *LGALS1* was observed to be significantly positively correlated with *LGALS3*, *SWAP70*, *CHI3L1*, *CCL2*, *SERPING1*, *ANXA1*, *SHC1*, *TIMP1*, *ICAM1*, *LTBP1*, *CD163*, *MR1* and *TNFRSF1A* (Fig. 5*d-f*).

Knockdown of *LGALS1* inhibits the GBM immunosuppressive microenvironment by down regulating M2 macrophages and MDSC cells, and inhibiting immunosuppressive cytokines

Using the TCGA and CGGA gene expression profiles, we observed that the M2 macrophage (CD68, CD163, CD204 and CD206)[25,26] and MDSCs (neutrophilic and monocytic) markers (CD14, CD15 and CD33)[27] had a positive relationship with *LGALS1* in GBM (Supporting Information Fig. S11A-H). The ELISA results revealed that knockdown of *LGALS1* decreased immunosuppressive cytokines such as CCL2, VEGFA and TGF-β (Fig. 6*a*). *In vitro* experiments, BV2 cells cultured with the glioma-conditioned medium (GCM) from cultured with GCM from GL261-NC cells had higher expression of Cd68, Cd163, Cd204 and Cd206 than those cultured with GCM from the GL261-*LGALS1*-si cells (Fig. 6*b*). The fraction of M2 macrophage ($CD68^+CD163^+$) and MDSC ($CD11b^+Gr\text{-}1^+$) cells in the tumour of tumour-bearing mice was reduced after knocking down *LGALS1* (Fig. 7*a-b*). Immunofluorescence results further revealed that M2 macrophage cells decreased after knocking down *LGALS1* (Fig. 7*c*). Finally, the immunohistochemistry-based quantifications of tumour sections also revealed a decreased presence of cytokines VEGFA, CCL2 and TGF-β and immunosuppressive cells, such as M2 macrophage (CD68 and CD163) and MDSC (CD11b) (Fig. 7*d*). These results suggested that *LGALS1* contributed to the GBM immunosuppressive microenvironment.

Discussion

GBM, the majority of malignant primary adult brain tumours, is a heterogeneous population comprising tumour cells, immune cells, and extracellular matrix, interactions among which expedite tumour development, progression and immune evasion.[28,29] The poor prognosis is a product of the transformed cells communicating with vascular cells, stromal cells and infiltrating inflammatory cells in tumour microenvironment.[30] In the present study, through the TCGA, CGGA, Rembrandt and GSE16011 databases, eight microenvironmental genes were identified by statistical analysis of data: *CCDC109B, EMP3, ANXA2, CLIC1, TIMP1, VIM, LGALS1* and *RBMS1*, which accounted for GBM microenvironment. The above eight genes were calculated so called the microenvironmental gene score. We found that chromosome 7 (EGFR) amplification accompanied with chromosome 10 loss (PTEN) occurred more frequent with the group with high glioma microenvironmental gene score. Most mutations of *IDH*1 and 1p/19q codeletion occurred in the group with low glioma microenvironmental gene score. All these findings implicated that glioma microenvironment was associated with specific genomic and transcriptomic spectrums indicating that they were biomarkers and potential therapeutic targets for glioma. Furthermore, we found that *LGALS1* revealed critical roles in remodelling the microenvironment and important clinical value in GBM. It revealed that *LGALS1* had a higher expression level in *IDH* wild-type GBM compared to that in *IDH* mutant GBM. It has been reported that *IDH* wild-type GBMs display a more prominent tumour infiltrating lymphocyte (TIL) infiltration and a higher PD-L1 expression than *IDH* mutant cases. *IDH1* wild-type GBM tissues include a statistically significant increased tendency of CD163 (M2 macrophage marker), PD1 and Foxp3 (Treg marker).[31] These results further implied that *LGALS1* might be involved in establishing an immunosuppressive microenvironment in GBM. Previous study showed that extracellular Galectin-1 encoded by *LGALS1* could modulate the survival time of tumour-infiltrating T cells by enhancing Fas ligand-induced apoptosis.[32] Galectin-1 deficiency increased CD3+ lymphocytes, CD4+ lymphocytes, CD8+ lymphocytes and decreased CD4+ Foxp3+ Tregs in GBM.[33] In pancreatic cancer, inhibition of Galectin-1 increased CD3+, CD4+, CD8+ lymphocytes but repressed CD11b + and Gr-1+ lymphocytes.[34] Galectin-1–deficient glioma cells could be eradicated by the infiltration of NK cells before the activation of the adaptive immune system.[35] The gene expression profiles from TCGA, CGGA, Rembrandt and GSE16011 databases contain expression spectrum of unselected cellular population including glioma cells and glioma-infiltrating immune cells. Heretofore, there have been few reports comprehensively illustrating the immunosuppressive status and genomic alterations in glioma with different *LGALS1* expression. Thus, deeply investigating the immune biological process of *LGALS1* based on current genomic databases may help to get a good idea of tumour immune complexity and guide potential anticancer immunotherapy. To investigate in detail how *LGALS1* was involved in the GBM immunosuppressive microenvironment, we undertook big data analysis and evaluated the immunosuppressive cytokines known to be tightly associated with immunosuppressive microenvironment. *LGASL1* was positively associated with immunosuppressive genes: *LGALS3*, impairing function of human CD4 and CD8 tumour-infiltrating lymphocytes,[36,37]

Figure 5. Immunosuppression is a predominate feature in GBMs with high *LGALS1* expression. (*a-c*) *LGALS1* was positively related to glioma-associated immunosuppressive metagenes, such as immunosuppressive cytokines and checkpoints, tumour-supportive macrophage chemotactic and skewing molecules, immunosuppressive signalling pathways, immunosuppressors, and markers of tregs. (*d*, *e*) Correlation of *LGALS1* and common immunosuppressive genes in GBM. [Color figure can be viewed at wileyonlinelibrary.com]

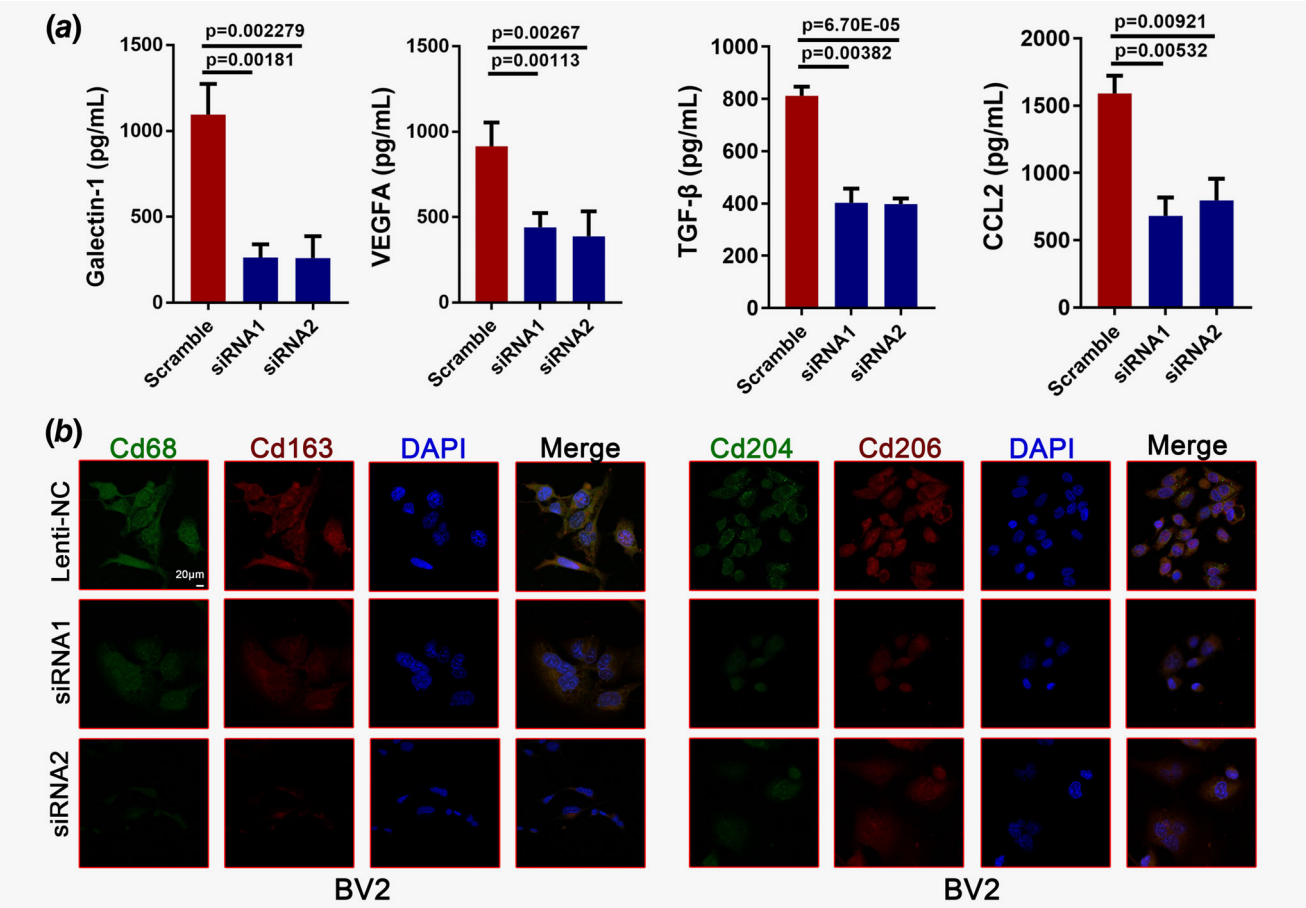

Figure 6. Knockdown of *LGALS1* inhibits the GBM immunosuppressive microenvironment *in vitro*. (*a*) ELISA assay was used to detect immunosuppressive cytokines, such as Galectin-1, CCL2, VEGFA and TGF-β in cell suspension. (*b*) Cd68, Cd163, Cd204 and Cd206 were stained after BV-2 cells were treated with GCM from the GL261-*LGALS1*-NC or GL261-*LGALS1*-si cells. [Color figure can be viewed at wileyonlinelibrary.com]

SWAP70 restricting spontaneous maturation of dendritic cells (DCs),[38,39] *CHI3L1* secreted by M2 macrophages promoting gastric and breast cancer metastasis,[40] *CCL2, SERPING1* inhibiting activation of the complement system,[41] *ANXA1* regulating TGF-β signalling and promoting metastasis formation of basal-like breast cancer cells,[42] *SHC1* promoting breast cancer immune suppression through STAT1 and STAT3,[43] *TIMP1* having a liner relationship with CD11b + Gr1+ myeloid cells and CD4 + CD25 + FOXP3+ Tregs,[37] *ICAM1* critical for mesenchymal stem cell (MSC)-mediated immunosuppression,[44] *LTBP1* required for an adequate TGF-β function,[45] *CD163, MR1* resulting in a relative increase in Tregs[4,46] *and TNFRSF1A* required for STAT3 phosphorylation and MDSC accumulation.[47] We also found that the expression of VEGFA, CCL2 and TGF-β were restrained in the *LGALS1* knockdown group. VEGFA promotes local and systemic immunosuppression and contributes to prevent the development of efficient antitumour immune responses. VEGFA/VEGFR-targeting therapies could revert such an immunosuppressive state.[48,49] Evidence shows that GBM expresses high levels of CCL2 and could contain high numbers of $CD14^+$ cells. Furthermore, the GBM supernatants could transform $CD14^+HLA\text{-}DR^+$ cells into $CD14^+HLA\text{-}DR^{lo/neg}$ immune suppressors.[50] TGF-β drives immune evasion and attenuates tumour response to PD-L1 blockade by contributing to exclusion of T cells.[51] TGF-β facilitates the immune suppressor capacity of high-grade glioma-derived $CD4^+CD25^+Foxp3^+$ T cells.[52]

Galectin-1 knockdown supresses glioma progression and improves the outcome of tumour-bearing mice.[53] Our bioinformatics results showed that there was a strong correlation among *LGALS1*, monocytes and myeloid lineage cells. We also observed the strong positive correlation between *LGALS1* and GBM-associated immunosuppressive cell markers of MDSC and M2 macrophages. M2 phenotype transformation occurs after IL-10, IL-4 and IL-13 exposure.[54] In GBM, M2 could be recruited by periostin secreted by glioblastoma stem cells (GSC) to participate in malignant growth.[55] M2 macrophages produce TGF-β,[56] contributing to a tumour-supporting and immunosuppressive environment in tumours.[57,58] Secretion of IL-10 and TGF-β were supressed after inhibition of *LGALS1*. The infiltration of M2 macrophages in the tumour site decreased after the knockdown of *LGALS1*. The same tendency was observed in

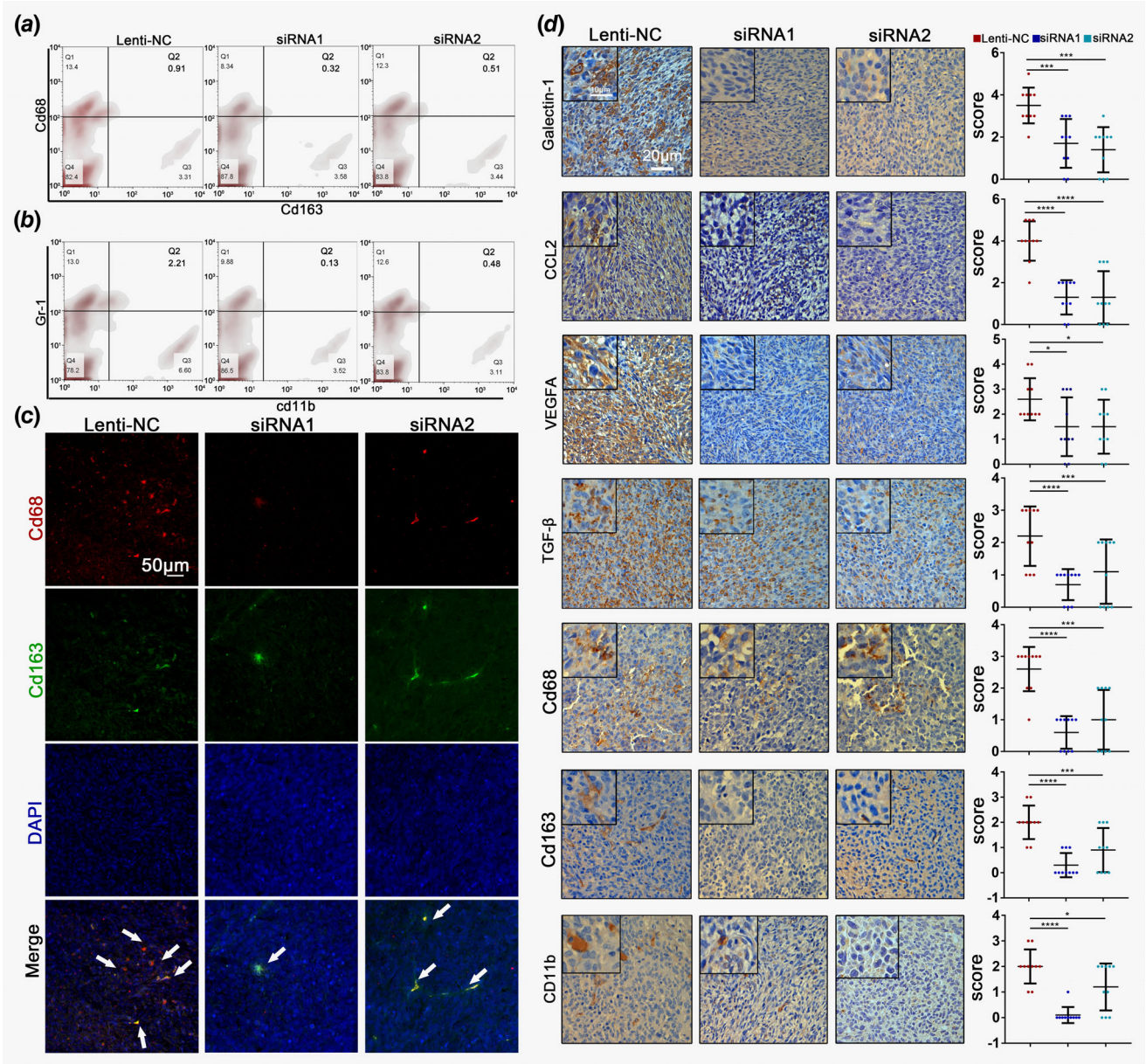

Figure 7. Knockdown of *LGALS1* inhibits the GBM immunosuppressive microenvironment *in vivo*. (*a*) The amount of M2 macrophages was measured by staining the cells isolated from the brains of tumour-bearing mice with anti-CD68 and anti-CD163. (*b*) The amount of MDSCs was measured by staining the cells isolated from the brains of tumour-bearing mice with anti-CD11b and anti-Gr-1. (*c*) In paraffin sections, the M2 macrophages were detected by costaining with M2 markers.(*d*) In paraffin sections, IHC was used to detect the immunosuppressive cytokines, such as Galectin-1, CCL2, VEGFA and TGF-β, and markers of M2 macrophage and MDSC. * $p < 0.05$, ** $p < 0.01$, *** $p < 0.001$, **** $p < 0.0001$. [Color figure can be viewed at wileyonlinelibrary.com]

MDSC cells, which are a heterogeneous set of cells of myeloid origin that can suppress T cell activity through the depletion of specific amino acids, which is essential for T-cell function.[59] In GBM, granulocytic MDSCs, a subset of MDSCs at the tumour site, play a major role in GBM-induced T-cell suppression.[60]

Conclusions

Our results thus implied an important role of microenvironmental regulation in glioma malignancy and provided evidences of *LGALS1* contributing to immunosuppressive environment in glioma by up regulating M2 macrophages and MDSC cells, and generating immunosuppressive cytokines. *LGALS1* could be a promising and potential therapeutic target, extending our understanding of anticancer immunotherapy in glioma.

Availability of data and materials

The databases supporting the conclusions of this article are included within the public databases TCGA, CGGA, Rembrandt, GSE16011 and GSE43378.

Ethics approval and consent to participate

The study involving human participants and animals was approved by the ethics committees of the Second Affiliated Hospital of Harbin Medical University, and all patients provided written informed consent.

References

1. Stupp R, Mason WP, van den Bent MJ, et al. Radiotherapy plus concomitant and adjuvant temozolomide for glioblastoma. *N Engl J Med* 2005;352:987–96.
2. Heimberger AB, Abou-Ghazal M, Reina-Ortiz C, et al. Incidence and prognostic impact of FoxP3+ regulatory T cells in human gliomas. *Clin Cancer Res* 2008;14:5166–72.
3. Louveau A, Smirnov I, Keyes TJ, et al. Structural and functional features of central nervous system lymphatic vessels. *Nature* 2015;523:337–41.
4. Doucette T, Rao G, Rao A, et al. Immune heterogeneity of glioblastoma subtypes: extrapolation from the cancer genome atlas. *Cancer Immunol Res* 2013;1:112–22.
5. Weathers SP, Gilbert MR. Current challenges in designing GBM trials for immunotherapy. *J Neurooncol* 2015;123:331–7.
6. Elola MT, Wolfenstein-Todel C, Troncoso MF, et al. Galectins: matricellular glycan-binding proteins linking cell adhesion, migration, and survival. *Cell Mol Life Sci* 2007;64:1679–700.
7. Astorgues-Xerri L, Riveiro ME, Tijeras-Raballand A, et al. Unraveling galectin-1 as a novel therapeutic target for cancer. *Cancer Treat Rev* 2014;40:307–19.
8. Vespa GN, Lewis LA, Kozak KR, et al. Galectin-1 specifically modulates TCR signals to enhance TCR apoptosis but inhibit IL-2 production and proliferation. *J Immunol* 1999;162:799–806.
9. Rubinstein N, Alvarez M, Zwirner NW, et al. Targeted inhibition of galectin-1 gene expression in tumor cells results in heightened T cell-mediated rejection; a potential mechanism of tumor-immune privilege. *Cancer Cell* 2004;5:241–51.
10. Wei JW, Cai JQ, Fang C, et al. Signal peptide peptidase, encoded by HM13, contributes to tumor progression by affecting EGFRvIII secretion profiles in Glioblastoma. *CNS Neurosci Ther* 2017;23:257–65.
11. Cai J, Chen Q, Cui Y, et al. Immune heterogeneity and clinicopathologic characterization of IGFBP2 in 2447 glioma samples. *Oncoimmunology* 2018;7:e1426516.
12. Sont JK, De Boer WI, van Schadewijk WA, et al. Fully automated assessment of inflammatory cell counts and cytokine expression in bronchial tissue. *Am J Respir Crit Care Med* 2003;167:1496–503.
13. Lambein K, Van Bockstal M, Vandemaele L, et al. Distinguishing score 0 from score 1+ in HER2 immunohistochemistry-negative breast cancer: clinical and pathobiological relevance. *Am J Clin Pathol* 2013;140:561–6.
14. Chen Q, Cai J, Wang Q, et al. Long noncoding RNA NEAT1, regulated by the EGFR pathway, contributes to Glioblastoma progression through the WNT/beta-catenin pathway by scaffolding EZH2. *Clin Cancer Res* 2018;24:684–95.
15. Bindea G, Mlecnik B, Hackl H, et al. ClueGO: a Cytoscape plug-in to decipher functionally grouped gene ontology and pathway annotation networks. *Bioinformatics* 2009;25:1091–3.
16. Subramanian A, Tamayo P, Mootha VK, et al. Gene set enrichment analysis: a knowledge-based approach for interpreting genome-wide expression profiles. *Proc Natl Acad Sci U S A* 2005;102:15545–50.
17. Yoshihara K, Shahmoradgoli M, Martinez E, et al. Inferring tumour purity and stromal and immune cell admixture from expression data. *Nat Commun* 2013;4:2612.
18. Barbie DA, Tamayo P, Boehm JS, et al. Systematic RNA interference reveals that oncogenic KRAS-driven cancers require TBK1. *Nature* 2009;462:108–12.
19. Gu Z, Gu L, Eils R, et al. Circlize implements and enhances circular visualization in R. *Bioinformatics* 2014;30:2811–2.
20. Krzywinski M, Schein J, Birol I, et al. Circos: an information aesthetic for comparative genomics. *Genome Res* 2009;19:1639–45.
21. Jin X, Kim LJY, Wu Q, et al. Targeting glioma stem cells through combined BMI1 and EZH2 inhibition. *Nat Med* 2017;23:1352–61.
22. Verhaak RG, Hoadley KA, Purdom E, et al. Integrated genomic analysis identifies clinically relevant subtypes of glioblastoma characterized by abnormalities in PDGFRA, IDH1, EGFR, and NF1. *Cancer Cell* 2010;17:98–110.
23. Case LD, Kimmick G, Paskett ED, et al. Interpreting measures of treatment effect in cancer clinical trials. *Oncologist* 2002;7:181–7.
24. Rody A, Holtrich U, Pusztai L, et al. T-cell metagene predicts a favorable prognosis in estrogen receptor-negative and HER2-positive breast cancers. *Breast Cancer Res* 2009;11:R15.
25. Glass R, Synowitz M. CNS macrophages and peripheral myeloid cells in brain tumours. *Acta Neuropathol* 2014;128:347–62.
26. Li W, Graeber MB. The molecular profile of microglia under the influence of glioma. *Neuro Oncol* 2012;14:958–78.
27. Raychaudhuri B, Rayman P, Ireland J, et al. Myeloid-derived suppressor cell accumulation and function in patients with newly diagnosed glioblastoma. *Neuro Oncol* 2011;13:591–9.
28. Ostrom QT, Bauchet L, Davis FG, et al. The epidemiology of glioma in adults: a "state of the science" review. *Neuro Oncol* 2014;16:896–913.
29. Cai J, Zhang W, Yang P, et al. Identification of a 6-cytokine prognostic signature in patients with primary glioblastoma harboring M2 microglia/-macrophage phenotype relevance. *PloS one* 2015;10:e0126022.
30. Hambardzumyan D, Gutmann DH, Kettenmann H. The role of microglia and macrophages in glioma maintenance and progression. *Nat Neurosci* 2016;19:20–7.
31. Rahman M, Kresak J, Yang C, et al. Analysis of immunobiologic markers in primary and recurrent glioblastoma. *J Neurooncol* 2018;137:249–57.
32. Matarrese P, Tinari A, Mormone E, et al. Galectin-1 sensitizes resting human T lymphocytes to Fas (CD95)-mediated cell death via mitochondrial hyperpolarization, budding, and fission. *J Biol Chem* 2005;280:6969–85.
33. Van Woensel M, Mathivet T, Wauthoz N, et al. Sensitization of glioblastoma tumor microenvironment to chemo- and immunotherapy by Galectin-1 intranasal knock-down strategy. *Sci Rep* 2017;7:1217.
34. Orozco CA, Martinez-Bosch N, Guerrero PE, et al. Targeting galectin-1 inhibits pancreatic cancer progression by modulating tumor-stroma crosstalk. *Proc Natl Acad Sci U S A* 2018;115:E3769–E78.
35. Baker GJ, Chockley P, Yadav VN, et al. Natural killer cells eradicate galectin-1-deficient glioma in the absence of adaptive immunity. *Cancer Res* 2014;74:5079–90.
36. Demotte N, Wieers G, Van Der Smissen P, et al. A galectin-3 ligand corrects the impaired function of human CD4 and CD8 tumor-infiltrating lymphocytes and favors tumor rejection in mice. *Cancer Res* 2010;70:7476–88.
37. Fukumori T, Takenaka Y, Yoshii T, et al. CD29 and CD7 mediate galectin-3-induced type II T-cell apoptosis. *Cancer Res* 2003;63:8302–11.
38. Quemeneur L, Angeli V, Chopin M, et al. SWAP-70 deficiency causes high-affinity plasma cell generation despite impaired germinal center formation. *Blood* 2008;111:2714–24.
39. Ocana-Morgner C, Gotz A, Wahren C, et al. SWAP-70 restricts spontaneous maturation of dendritic cells. *J Immunol* 2013;190:5545–58.
40. Chen Y, Zhang S, Wang Q, et al. Tumor-recruited M2 macrophages promote gastric and breast cancer metastasis via M2 macrophage-secreted CHI3L1 protein. *J Hematol Oncol* 2017;10:36.
41. Fornvik K, Maddahi A, Persson O, et al. C1-inactivator is upregulated in glioblastoma. *PLoS one* 2017;12:e0183086.
42. de Graauw M, van Miltenburg MH, Schmidt MK, et al. Annexin A1 regulates TGF-beta signaling and promotes metastasis formation of basal-like breast cancer cells. *Proc Natl Acad Sci U S A* 2010;107:6340–5.
43. Ahn R, Sabourin V, Bolt AM, et al. The Shc1 adaptor simultaneously balances Stat1 and Stat3 activity to promote breast cancer immune suppression. *Nat Commun* 2017;8:14638.
44. Ren G, Zhao X, Zhang L, et al. Inflammatory cytokine-induced intercellular adhesion molecule-1 and vascular cell adhesion molecule-1 in mesenchymal stem cells are critical for immunosuppression. *J Immunol* 2010;184:2321–8.
45. Caja L, Dituri F, Mancarella S, et al. TGF-beta and the tissue microenvironment: relevance in fibrosis and cancer. *Int J Mol Sci* 2018;19.
46. Vogel I, Verbinnen B, Van Gool S, et al. Regulatory T cell-dependent and -independent mechanisms of immune suppression by CD28/B7 and CD40/CD40L costimulation blockade. *J Immunol* 2016;197:533–40.
47. Sobo-Vujanovic A, Vujanovic L, DeLeo AB, et al. Inhibition of soluble tumor necrosis factor prevents chemically induced carcinogenesis in mice. *Cancer Immunol Res* 2016;4:441–51.
48. Terme M, Tartour E, Taieb J. VEGFA/-VEGFR2-targeted therapies prevent the VEGFA-

induced proliferation of regulatory T cells in cancer. *Oncoimmunology* 2013;2:e25156.
49. Schmittnaegel M, Rigamonti N, Kadioglu E, et al. Dual angiopoietin-2 and VEGFA inhibition elicits antitumor immunity that is enhanced by PD-1 checkpoint blockade. *Sci Transl Med* 2017;9: eaak9670.
50. Gustafson MP, Lin Y, New KC, et al. Systemic immune suppression in glioblastoma: the interplay between CD14+HLA-DRlo/neg monocytes, tumor factors, and dexamethasone. *Neuro Oncol* 2010;12:631–44.
51. Mariathasan S, Turley SJ, Nickles D, et al. TGFbeta attenuates tumour response to PD-L1 blockade by contributing to exclusion of T cells. *Nature* 2018;554:544–8.
52. Liang H, Yi L, Wang X, et al. Interleukin-17 facilitates the immune suppressor capacity of high-grade glioma-derived CD4 (+) CD25 (+) Foxp3 (+) T cells via releasing transforming growth factor beta. *Scand J Immunol* 2014;80:144–50.
53. Verschuere T, Toelen J, Maes W, et al. Glioma-derived galectin-1 regulates innate and adaptive antitumor immunity. *Int J Cancer* 2014;134: 873–84.
54. Mantovani A, Sozzani S, Locati M, et al. Macrophage polarization: tumor-associated macrophages as a paradigm for polarized M2 mononuclear phagocytes. *Trends Immunol* 2002;23: 549–55.
55. Zhou W, Ke SQ, Huang Z, et al. Periostin secreted by glioblastoma stem cells recruits M2 tumour-associated macrophages and promotes malignant growth. *Nat Cell Biol* 2015;17:170–82.
56. Balkwill F, Charles KA, Mantovani A. Smoldering and polarized inflammation in the initiation and promotion of malignant disease. *Cancer Cell* 2005; 7:211–7.
57. Byrne SN, Knox MC, Halliday GM. TGFbeta is responsible for skin tumour infiltration by macrophages enabling the tumours to escape immune destruction. *Immunol Cell Biol* 2008;86:92–7.
58. Ahmadzadeh M, Rosenberg SA. TGF-beta 1 attenuates the acquisition and expression of effector function by tumor antigen-specific human memory CD8 T cells. *J Immunol* 2005;174:5215–23.
59. Gabrilovich DI, Nagaraj S. Myeloid-derived suppressor cells as regulators of the immune system. *Nat Rev Immunol* 2009;9:162–74.
60. Dubinski D, Wolfer J, Hasselblatt M, et al. CD4+ T effector memory cell dysfunction is associated with the accumulation of granulocytic myeloid-derived suppressor cells in glioblastoma patients. *Neuro Oncol* 2016;18:807–18.